Characterization of chert in the Dammam Formation (Eocene), Kuwait: Clues to groundwater silicification processes

Fikry Ibrahim Khalaf, Médard Thiry, Anthony Milnes, Rehab Alnaqi

Journal of Sedimentary Research

Journal of Sedimentary Research, 2020, v. 90, 297–312
Research Article
DOI: http://dx.doi.org/10.2110/jsr.2020.18

CHARACTERIZATION OF CHERT IN THE DAMMAM FORMATION (EOCENE), KUWAIT: CLUES TO GROUNDWATER SILICIFICATION PROCESSES

FIKRY IBRAHIM KHALAF,*[1] MÉDARD THIRY,[2] ANTHONY MILNES,[3] AND REHAB ALNAQI[1]
[1]*Department of Earth and Environmental Sciences, Faculty of Science, Kuwait University, P.O. Box 5969, Safat 13060, Kuwait*
[2]*MINES ParisTech, PSL Research University, Centre of Geosciences, 35 rue St. Honoré, 77305 Fontainebleau, Cedex, France*
[3]*Department of Earth Sciences, The University of Adelaide, North Terrace, Adelaide, 5005, South Australia*
e-mail: medard.thiry@mines-paristech.fr

ABSTRACT: **Conspicuous chert horizons occur as discontinuous bands and isolated nodules in dolostones in the Eocene Dammam Formation, which is exposed in the southeast of Kuwait. The Formation has never been deeply buried, and so chert formation is likely to have resulted from silicification processes at or near the land surface. Erosional reworking of the chert constrains its formation to a time period between the late Eocene and the Mio-Pliocene. As there is no significant source of silica in the dolostones, the chert was formed from silica imported from other sources. This process, together with the specificity of chert to particular non-bedding horizons, suggests that silicification is related to discrete locations of the groundwater table during landscape incision and resultant groundwater discharge in the region. Detailed petrographical studies demonstrate that "chertification" was initiated by precipitation of nanoglobules of silica (opal-A) from supersaturated groundwater solutions flowing through voids formed concomitantly by dissolution of dolomite. Subsequently, silica was precipitated as more crystalline forms of chalcedony, microquartz, and megaquartz from successively less saturated groundwater. The most likely mechanism for triggering the precipitation of silica is considered to be significant cooling of the groundwater as it neared the landsurface and came into contact with a cold regolith terrain. Precipitation of disordered forms of silica (opal-A) occurred at the cold front: progressively more crystalline phases formed as the host rock was warmed by the inflowing groundwater and its degree of supersaturation diminished. If our interpretation is correct, this "chertification" process could have been initiated during global cooling related to one of the glaciations recorded during Oligocene and Miocene times.**

INTRODUCTION

Siliceous nodular masses that preserve depositional and diagenetic textures and structures are common in limestone and dolostone. They are generally referred to as chert, especially when they occur in marine formations that may or may not have undergone burial diagenesis (Maliva and Siever 1988a), and can also be referred to as silicified limestone and dolostone or silicified calcrete when occurring in shallow water and/or in continental deposits (Cayeux 1929; Nash and Shaw 1998; Arakel et al. 1989; Thiry and Ribet 1999). Herein the term "chert" is used without any genetic connotation for completely and partially silicified carbonate rocks.

Early studies of chert date back to the end of the 19th century, at about the same time as the development of optical microscopy. The founding petrological works raised problems with the origin of the silicification and related silica transfer processes. In thick marine series with chert and flint layers, epigenetic replacement of the primary calcareous matrix was highlighted as well as the role of siliceous organisms as a source of silica. Hypotheses were formulated for silica migration by diffusion and its concentration in particular horizons during early or deep diagenesis (Van Tuyl 1918; Cayeux 1929; Biggs 1957). In thinner, shallow continental sequences, which were never deeply buried, silica deposits in vugs and dissolution features are common. In this case, silica was considered to be imported to the host formation by circulating water (Storz 1926; Kaiser 1928; Cayeux 1929). However, knowledge of silica geochemistry was lacking in these pioneer works. Evaporation was usually proposed as the mechanism to concentrate waters and precipitate silica. It is from this time that silicification of continental formations was ascribed to hot and dry climates, most frequently during deposition of the host sediment (Fersmann and Wlodawetz 1926; Alimen 1936; Alimen and Deicha 1959; Arbey 1980; Daley 1989). The conclusions of a study of the origin of early and late cherts in the Leadville Limestone, Colorado (Banks 1970) summarize the generally held view that "... late cherts appear to have precipitated from groundwaters as amorphous silica after initial lithification ... super-saturation probably was obtained by evaporative concentration at the water–air interface during dry seasons ... and dissolution of the limestone by slightly acid waters may account for the removal of the calcite that is replaced by chert." These approaches formed the paradigm that supported the study of near surface silicification during the 20th Century.

Later studies of various formations and contexts, together with better knowledge of silica geochemistry, including quantitative aspects, geochemical modeling, and dating, profoundly changed the concepts of subsurface silicification. Among the new hypotheses, silica precipitation

* Present Address: Geology Department, Faculty of Science, Port-Said University, 24 December Street, Port-Said, Egypt

Published Online: March 2020

FIG. 1.—Location map. Dolostone quarry, located about 10 km from the Arabian Gulf shore.

from groundwater in response to cooling has been proposed recently for some case studies (Alexandre et al. 2004; Thiry et al. 2015a, 2015b; Thiry and Milnes 2017). Cooling is a powerful factor for initiating silica precipitation from solution and, contrary to solution concentration by evaporation, it allows renewal of the solution and thus silica supply while silica solubility decreases. This point of view puts into question a number of former paleoclimatic interpretations of surficial and subsurface silicification. Moreover, it suggests that near-surface groundwater silicification in continental realms could be used as a proxy for climate cooling events.

The present study of the chert in the Eocene Dammam Formation in Kuwait was undertaken with these new concepts in mind. Nodular silica segregations in Dammam Formation dolostones display a wide variation in their mode of occurrence, mineralogical composition, and petrographical characteristics. As such, they provide a strong base for interpreting the factors that controlled their mode of occurrence and formation.

GEOLOGICAL SETTING

The chert studied herein occurs in the lower Eocene to early upper Eocene Dammam Formation. This constitutes the upper part of the Paleocene–Eocene Hasa Group succession, which is extensively exposed in the eastern parts of the Arabian platform (Powers et al. 1966; Al-Awadi et al. 1998; Sander 2012; Tanoli and Al-Bloushi 2017). In the subsurface of Kuwait, the Dammam Formation is represented by a sequence of limestones and dolostones that varies in thickness from 150 m in the southeast to 275 m in the northeast. It is unconformably overlain by the Mio-Pleistocene Kuwait Group siliciclastic sequence, which may reach up to 200 m thickness (Owen and Nasr 1958).

The upper part of the Dammam Formation is exposed in a quarry (Al Ahmadi quarry) located in the southeast of Kuwait on the Ahmadi anticline (Fig. 1). The Al Ahmadi quarry occupies an area of approximately 2 km^2 atop the greater Burgan oilfield. Here, the upper member of the Dammam Formation is partly exposed as an approximately 20-m-thick section of chert-rich dolostone (Fuchs et al.1968; Khalaf et al. 1989) separated by a karstic erosion surface from an overlying relatively thin sequence of undifferentiated Kuwait Group siliciclastics (Burdon and Al-Sharhan 1968).

FIELD RELATIONSHIPS

Dammam Formation Dolostones

The dolostone sequence hosting the chert is whitish, porous, and friable (chalky) at the base and grades upwards into a hard dense dolostone (Fig. 2). The basal unit is exposed in a rock wall approximately 12 m high in the western side of the quarry. It is thick-bedded (beds up to 1.5 m with well-defined bedding planes) and fossiliferous with laminated interbeds of dense dolomicrite up to 0.5 m in thickness. The upper unit reaches 8 m in thickness and is an extensively fractured and karstified dense dolostone with vuggy and cavernous porosity. The bedding arrangement and sedimentary facies are similar to that of the chalky dolostone, but the contact between the chalky dolostone and the hard dolostone is commonly uneven and imprecise. The hard dolostone is considered to have formed by alteration and recrystallization of the chalky dolostone (Khalaf et al. 2018).

The contact with the overlying Kuwait Group siliciclastics is an irregular karstified erosion surface (Fig. 2) marked by a thin, discontinuous band of lag material, including abundant chert fragments and locally reworked and rounded chert cobbles. Clearly, the top of the Dammam Formation dolostone was karstified before being buried by the Kuwait Group siliciclastic deposits (Khalaf et al. 1989).

Chert

Occurrence.—In the chalky dolostone, chert occurs mostly as discontinuous bands that reach 40 cm in thickness and extend for several tens of meters along horizons that are slightly discordant to bedding. Some horizons of isolated chert nodules are more closely aligned to bedding planes. The chert is massive and hard, and varies in color, but is mostly dull gray. Extensive chert bands are associated with thinly laminated, dense dolomicrite horizons, and some chert encloses remnants of the host dolostone. In the karstic hard dolostone, the chert does not occur in extended bands but more commonly as discrete chert lumps a few centimeters in size.

There is a significant variation in the abundance of chert in the quarry profile, with more chert nearer the top of the profile in the karstic hard dolostone and the upper part of the chalky dolostone (Fig. 2).

Morphology.—Nodular chert mostly occurs in the lower chalky dolostone unit as isolated masses. It is commonly of irregular shape (oblate to ellipsoidal, ratio of length to thickness from 2 to 5) and varies in size from few centimeters to more than 30 cm (Fig. 3A). Spherical nodules are rare. Nodular chert also occurs in the hard dolostone.

Thin bands of chert up to 5 cm thick and extending discontinuously for less than a meter occur frequently in horizons within the chalky dolostone facies. The chert bands mostly have flat to slightly undulating top and bottom surfaces, but a few have jagged borders due to irregular silicification of the surrounding host rock. In some slightly laminated dolostone horizons, banded chert occurs as discontinuous patches that extend towards each other or are welded to form a more extended band (Fig. 3B). Irregular, amoeboid-shaped chert bodies (Fig. 3C) reaching tens of centimeters in size are chaotically scattered within the hard dolostone in places and also occasionally occur within the chalky dolostone. They can enclose remnants of host dolostone; if the dolomite has dissolved, this confers a cavernous aspect highlighting the complex interpenetrating contacts between dolomite and chert (Fig. 3D).

Most of the chert masses have a homogeneous internal structure without distinctive elements. However, some display specific structures and textures that provide clues to their mode of formation. For example,

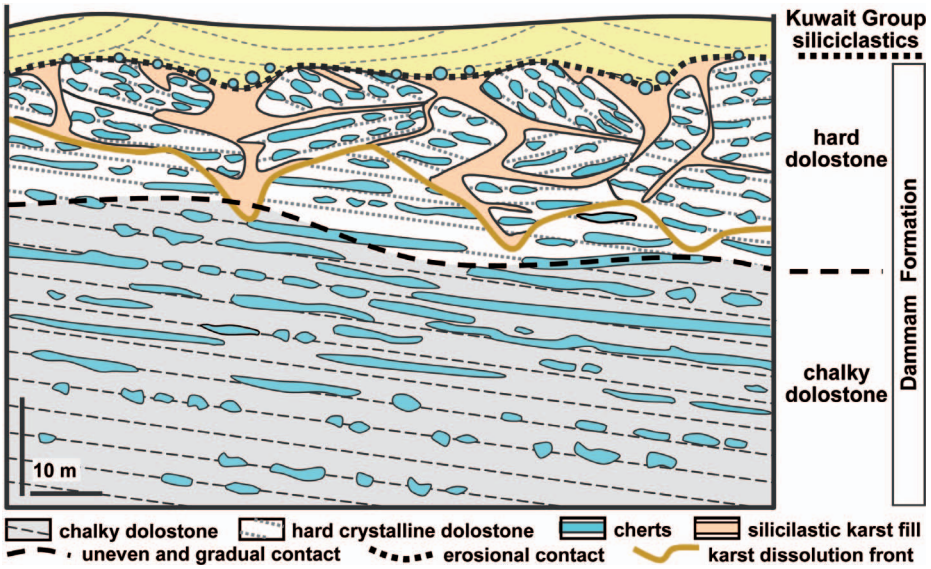

FIG. 2.—Lithostratigraphic sketch of Al Ahmadi quarry (southeast of Kuwait). Geometrical arrangements indicate successively: (1) recrystallization of upper chalky dolostone into hard dolostone along an uneven contact; (2) chert development through this contact but slightly discordant with bedding, and an upward increase in degree of silicification; (3) karstification of the dolostone formation; and (4) capping of the section by siliciclastic deposits. Thickness of chert masses has been enhanced in this diagram.

porous chert bands are common within porous grainstone dolomicrite, but whether the porosity is primary or results from the dissolution of residual carbonate elements after silicification is not known. "Ghost" structures inherited from the host dolostone include remnants of laminae, carbonaceous or silicified allochems (pelecypod shells, peloids, and intraclasts), cracks, and voids. Homogeneous fabric and "ghost" structures may occur in the same chert mass whereby the remnant usually occupies the interior of the mass.

The boundaries between the chert and the dolostone may be more or less sharp or transitional with a friable cortex. In the case of chert within the chalky dolostone, transitional boundaries that tend to match the smooth, undulatory contours of the chert mass are typical and vary in width from a few millimeters to centimeters. Sharp boundaries are also observed and are mostly smooth but may be corrugated. Irregular boundaries with indented contours are the most frequent type, and generally characterize the chert in porous and vuggy dolostone and dolocrete.

Sedimentary and Diagenetic History of Dammam Formation Dolostones.—Features observed in the Al Ahmadi quarry allow us to reconstruct the sedimentary and diagenetic history of this part of the sequence, as shown schematically in Figure 2.

- The Dammam Formation dolostones were originally deposited in a tidal flat and backshore embayment and were pervasively dolomitized penecontemporaneously with sedimentation (Khalaf et al. 2018).
- After regression of the sea, the chalky dolostone deposits in the upper part of the sequence were altered and recrystallized to form hard crystalline dolostone (Khalaf 2007).
- Chert formation followed, as is indicated by the silicification of dolosparite crystals characteristic of the hard dolostone.
- Karst developed after chert formation, as demonstrated by the lag of reworked chert clasts within the siliciclastic infills of karst cavities and on the unconformity surface at the base of the overlying Kuwait Group sediments.

The sequence was never covered by a substantial overburden, as attested by the nature of the Kuwait Group deposits (Al-Awadi et al. 1998; Al-Sulaimi and Al-Ruwaih 2004) and the lack of compaction of the primary grainstone and packstone fabric (Khalaf et al. 2018). All diagenetic alterations and transformations are considered to have occurred in near-surface or shallow subsurface environments.

PETROGRAPHY

Alteration of Dolostone to Chert

Degree of Silicification.—Variations in the degree of silicification of dolostone to chert are reflected in the gross chemistry and mineralogy of the studied samples (Table 1). For example, chemical analyses indicate that chert in the chalky dolostone contains around 57–73% SiO_2 compared with around 26–55% SiO_2 in the hard dolostone. This is confirmed by XRD analyses showing more abundant quartz in chert in the chalky dolostone (average $\sim$ 79%) than in the hard dolostone (average $\sim$ 64%). Moreover, chemical and XRD data are in agreement and indicate 10–35% dolomite in chert in the chalky dolostone compared with 25–60% in chert in the hard dolostone. Petrographic observations show that the higher abundance of dolomite in chert in the hard dolostone is accounted for by the frequency of remnants of limpid and euhedral dolomite crystals scattered within the silica matrix. Al, Fe, K, and S occur in trace amounts in all chert samples.

Boundaries between Chert and Dolostone.—The petrography of chert samples shows various degrees of silicification of host dolostone from partial to complete alteration. The formation of chert was initiated by the infilling of vugs, channels, and fossil mold cavities with silica deposited from solution (Fig. 4A) and continued via progressive pervasion of dolostone by solution and replacement of the dolomitic groundmass by silica along a relatively sharp diffusion boundary (Fig. 4B). The transitional zone between chert and host dolostone can vary in width from a few millimeters to centimeters. In places, remnants of the host dolostone occur in the chert as light gray to buff-color "ghosts." The geometrical characteristics of the silica-filled voids clearly identify them as micro-karst dissolution features (Fig. 4A).

Complete silicification of dolostone involved the infilling of voids and replacement of the dolomitic groundmass as well as the dolomitic allochems (Fig. 4C) and resulted in sharp boundaries between chert and host. Vugs, or rather fossil mold cavities, are occasionally preserved in the bordering dolostone without any silica infillings. The result is a dark gray-black homogeneous chert in which there is no residual texture of the parent dolostone, all former textures and structures having been obliterated.

Characterization of Silica in Chert.—The distribution and succession of various silica polymorphs in the Dammam Formation chert can be

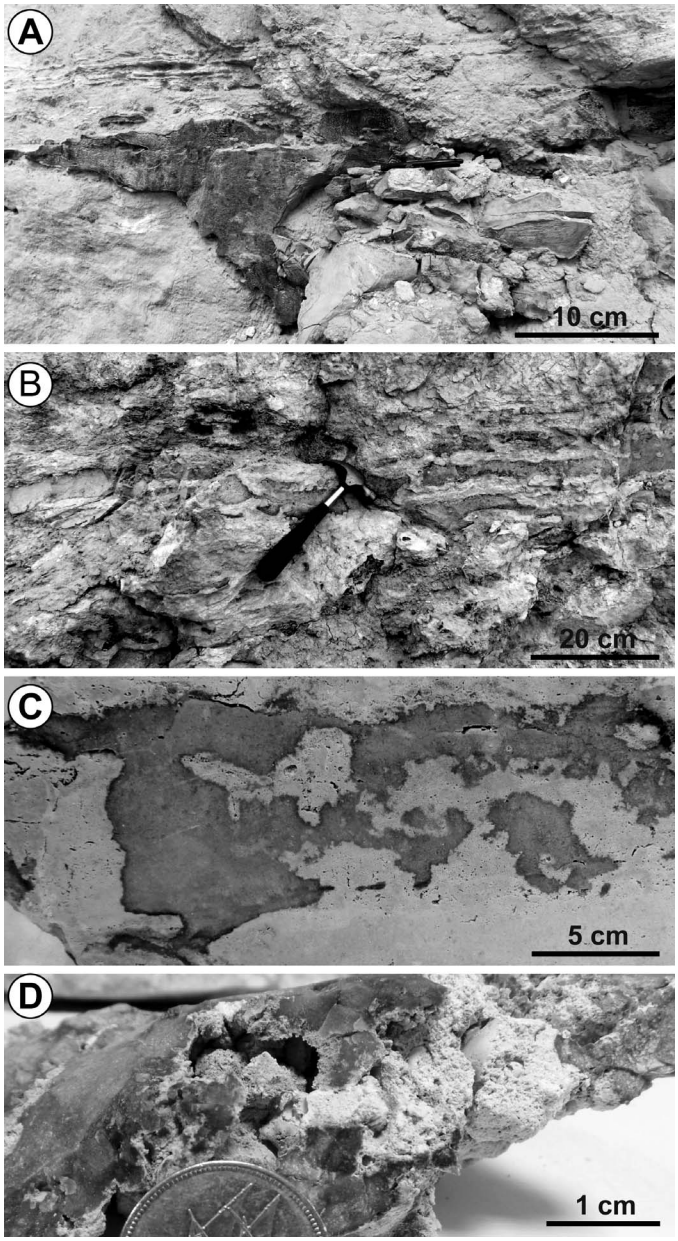

FIG. 3.—Chert disposition in dolostone. **A)** Chert band with sharp, even top and corrugated bottom partially replacing thin bed of laminated chalky dolostone. **B)** Discontinuous chert band with irregular contours within hard dolostone. **C)** Irregular, amoeboid-shaped chert bodies within hard crystalline dolostone. **D)** Cavernous chert as it appears when remnant dolomite has been dissolved.

readily identified in thin sections. These observations are keys to unravelling mechanisms of silica importation and deposition, particularly the temporal sequence of silica deposition and transformation of the silica polymorphs.

Forms of Silica.—Four main silica polymorphs are recognized in the chert samples and from the most poorly organized to the most crystalline forms are: opal, chalcedony, microcrystalline quartz, and megaquartz. In this study we adopted the terminology and the optical and morphological characteristics of fibrous silica polymorphs of Mallard (1890) and Michel-Levy and Munier-Chalmas (1892) as summarized by Arbey (1980), based on French samples from surface paleoenvironments. This is in agreement with the Hendry and Trewin (1995) classification of fibrous silica polymorphs known from deeper burial environments. Scanning electron microscopy (SEM) provided complementary information on the morphological and spatial relationships between silica polymorphs.

- **Opal-A and opal-CT** are not easily recognized by optical microscopy, but thin isotropic and light brownish colored laminae approximately 10 μm thick lining fractures and voids within some samples are interpreted as opal-A (Fig. 5A).
- **Chalcedony** commonly forms botryoidal or mammillary wall linings (up to 1 mm thick) of cavities and channels and consists of micro-laminated and juxtaposed sheaves and spherolites. Length-fast chalcedony is the most common variety (Fig. 5B). In addition there are length-slow chalcedony pseudomorphs with regular extinction along fibers, or variable birefringence along a single fiber due to the rolling-up of fibers around the Nε index and appear as indented zones, alternately light and extinct (Fig. 5C), called zebraic- or twisted-chalcedonite according to Chowns and Elkins (1974) and Arbey (1980). The fibrous structure appears only if the sheaves are cut (by the thin section) along their axis: if perpendicular to their axis, chalcedony at the termination of the fibers looks like microquartz.
- **Microcrystalline quartz** (microquartz) is the most abundant silica polymorph and commonly occurs as subeuhedral to xenomorphic mosaics of randomly oriented crystals < 20 μm in size, the largest of which display undulatory extinction. At around 5μm in size their birefringence is very low, and smaller crystals appear to be isotropic (extinguished). Domains of microcrystalline quartz are mostly homogeneous without any particular structure. Structures in the parent dolostone, including dolomite crystal remnants, fossils, laminations, voids, and cracks generally control the distribution of microcrystalline quartz.
- **Megaquartz** crystals have a crystal size greater than 20 μm. Isometric and elongated crystals are the two main types, and both may be euhedral or xenomorphic. The most common isometric megaquartz forms equant mosaics that constitute the ultimate filling of cavities (Fig. 5D). They generally have a sharp extinction and exhibit planar boundaries between groups of three crystals, each having grown by the same increment. They may also occur in a jigsaw arrangement with an imbricate sinuous outline. Elongated quartz crystals form palisadic or comb-like arrangements and are generally implanted normally on a surface with their optical axes subparallel (Fig. 5E). Another frequent arrangement, termed petaloid, shows the radial distribution of quartz crystals around a center of crystallization (Fig. 5F). Extinction of petaloid quartz crystals is often feathery (Fig. 5G) or flamboyant (Fig. 5H), and most are length-slow. They may display one or more poorly individualized fiber directions and have euhedral terminations of cubic appearance and uniform extinction (Fig. 5I; Milliken 1979; Arbey 1980).

Void Fillings of Silica.—Silica infilling pores and cavities shows several patterns of multiple textures of various silica polymorphs. These are mostly various sizes and fabrics of normal and feathery quartz crystals as well as chalcedony. The fillings usually gradually increase in size from microquartz lining the void walls to large euhedral silica polymorphs that represent the final phase of crystallization towards the center of the void.

Most commonly, silica infilling voids occurs as laminae (each 10 to 15 μm thick) lining the cavity walls. The initial laminae are composed of elongated flamboyant microquartz that grade inwards to small flamboyant palisadic quartz arranged perpendicular to the void walls (Fig. 6A). The final lamina is often surmounted by a layer of palisadic quartz with euhedral tips. Towards the centers of the voids, the palisadic quartz grades into mosaics of equant subeuhedral and euhedral macroquartz crystals

TABLE 1.—*Chemical and mineralogical composition of chert samples. Chemical and mineralogical analyses were carried on about 3–5 cm³ volume of ground sample in order to average heterogeneity of dolomite remnants.*

	Concentration % of Major Oxides - XRF										Chem. Calculation		Mineral% - XRD	
Sample	SiO_2	CaO	MgO	Na_2O	K_2O	Al_2O_3	Fe_2O_3	SO_3	SrO (ppm)	LOI	CaO/MgO	dolomite	quartz	dolomite
chertified chalky dolostone														
R1	59.75	10.13	5.12	1.8	0	0.04	0.87	0.03	34	22.25	1.97	20.78	75	25
R2	71.07	5.99	3.63	1.43	0.02	0.06	0.94	0.04	40	16.80	1.65	14.74	80	20
R3	60.12	8.08	4.48	2.77	0.02	0.05	0	0.07	29	24.25	1.96	18.19	80	20
R4	61.1	8.50	5.18	2.13	0.02	0.07	0.9	0.06	46	22.02	1.64	21.03	75	25
R5	56.6	11.55	6.44	2.24	0.02	0.07	0.63	0.05	49	22.29	1.79	26.15	65	35
R6	70.45	5.57	3.13	2.56	0.02	0.07	0.81	0.04	22	17.40	1.75	12.71	85	15
R7	73.01	3.57	2.13	3.36	0.01	0	0.79	0.03	22	17.00	1.67	8.65	90	10
maximum	73.01	11.55	6.44	3.36	0.02	0.07	0.94	0.07	49	24.25	1.97	26.15	65	35
minimum	56.6	3.57	3.13	1.43	0	0	0	0.03	22	16.80	1.64	8.65	90	10
average	64.6	7.60	4.300	2.30	0.0	0.05	0.71	0.0	34.6	20.30	1.77	15.64	78.6	21.4
chertified karst dolostone														
K1	54.93	8.5	6.11	3.3	0.02	0.09	0.48	0.04	38	26.40	1.39	24.81	75	25
K2	42.88	11.84	8.37	3.78	0.02	0.07	0.47	0.06	51	31.67	1.41	33.98	65	35
K3	41.51	12.01	8.89	3.87	0.02	0.07	0.7	0.04	47	32.05	1.35	36.09	70	30
K4	51.58	12.66	8.57	3.02	0.01	0.06	0.69	0.05	53	22.75	1.47	34.79	75	25
K5	42.36	14.67	9.48	1.86	0.02	0	0.55	0.07	64	30.51	1.54	38.49	60	40
K6	26.43	18.96	13.12	1.85	0.01	0.05	0.17	0.1	0	38.99	1.44	53.66	40	60
K7	49.78	14.25	10.12	1.34	0.02	0.08	0.54	0.09	65	23.40	1.43	41.08	60	40
maximum	54.93	18.96	13.12	3.87	0.02	0.09	0.7	0.1	65	38.99	1.44	53.66	75	60
minimum	26.43	8.50	6.11	1.34	0.01	0	0.17	0.04	0	22.75	1.39	24.81	40	25
average	44.2	13.3	9.20	2.70	0.0	0.06	0.51	0.1	45.4	29.40	1.43	37.55	63.6	36.4

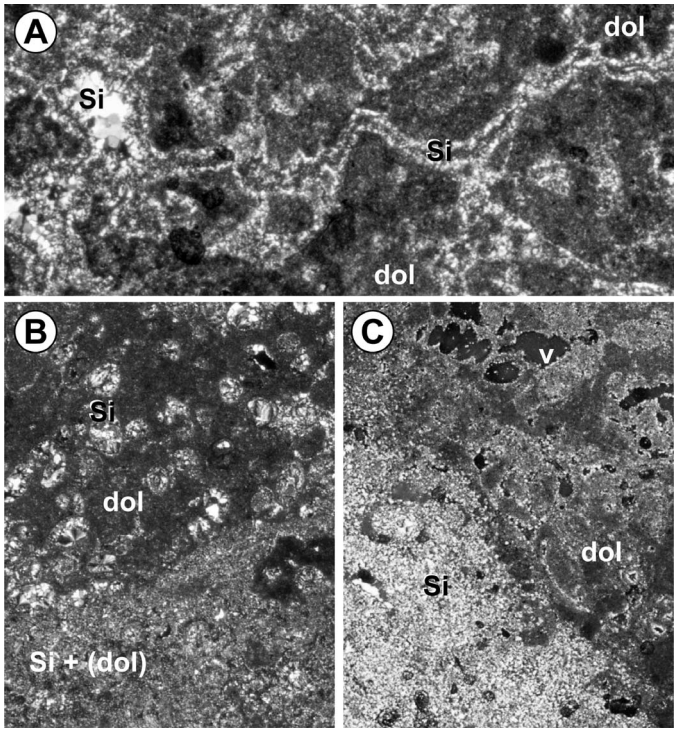

FIG. 4.—Micrography of transformation from dolostone to chert. **A)** Silica infilled micro-karst dissolution features. Silica is restricted to vugs. Dark dolostone groundmass does not contain silica. **B)** Transitional boundaries composed of dolostone rim composed of fossil mold voids filled with silica and chert rim with dolostone remnants. **C)** Sharp boundary with silicification in dolomite. Note absence of silica deposits in gastropod mold cavities whereas in advanced stages of chertification voids are silica filled and dolomitic groundmass replaced by quartz with dolomite "ghost" structures preserved. Crossed nicols. dol, dolostone; Si, silica; v, vug.

(Fig. 6A′) or occasionally to a crystal mosaic with imbricate sinuous outline and undulatory extinction.

There are many variations in morphology, size, and extinction of silica laminae. Chessboard extinction along the laminae points to alternating length-fast and length-slow elongated quartz crystals. In places, opal laminae occur between laminae of microquartz or flamboyant palisadic quartz (Fig. 6B).

Uniform laminae of silica that mimic the contours of the walls of voids, and in which there is a gradation in crystal size, are the most common. However, some voids, particularly some fossil molds and a few dissolution voids, are infilled by laterally stacked, mamillated, length-fast chalcedony spherules or sheaves with sharp, straight contacts (Fig. 6C). Each sheaf consists of radially arranged microfibers that originate at a small number of points along the walls of the cavities, suggesting initial precipitation at discrete nucleation centers (Fig. 6D). The sheaves are more than 300 μm long and display successive extinction banding, which is sometimes oscillatory with two or three thin bands (around 5 μm) alternating with thick bands (around 50 μm). The banding arrangement clearly shows that silica was not deposited along the void walls, but that the sheaf-like spherules developed in euhedral fashion by crystalline growth. In most voids, spherules of chalcedony form the initial wall coatings, and the remaining fill is a mosaic of subeuhedral megaquartz crystals (Fig. 6D). Sheaves of chalcedony may cluster together and display intricate relationships due to the tortuous morphology of the void. In some voids, groups of sheaves may be formed of zebraic or twisted chalcedony (Fig. 5C) and even of feathery megaquartz (Fig. 5G) and radiant petaloid megaquartz (Fig. 5F).

The occurrence of voids lined with laminated deposits of silica is variable. Small voids may be completely infilled with laminated silica deposits, especially at the margins of large cavities, but the laminated deposits may disappear away from these large cavities (Fig. 6F). Other voids may contain only a thin film of silica, or none at all, particularly in the case of fossil mold voids (Fig. 6E). In these examples, euhedral

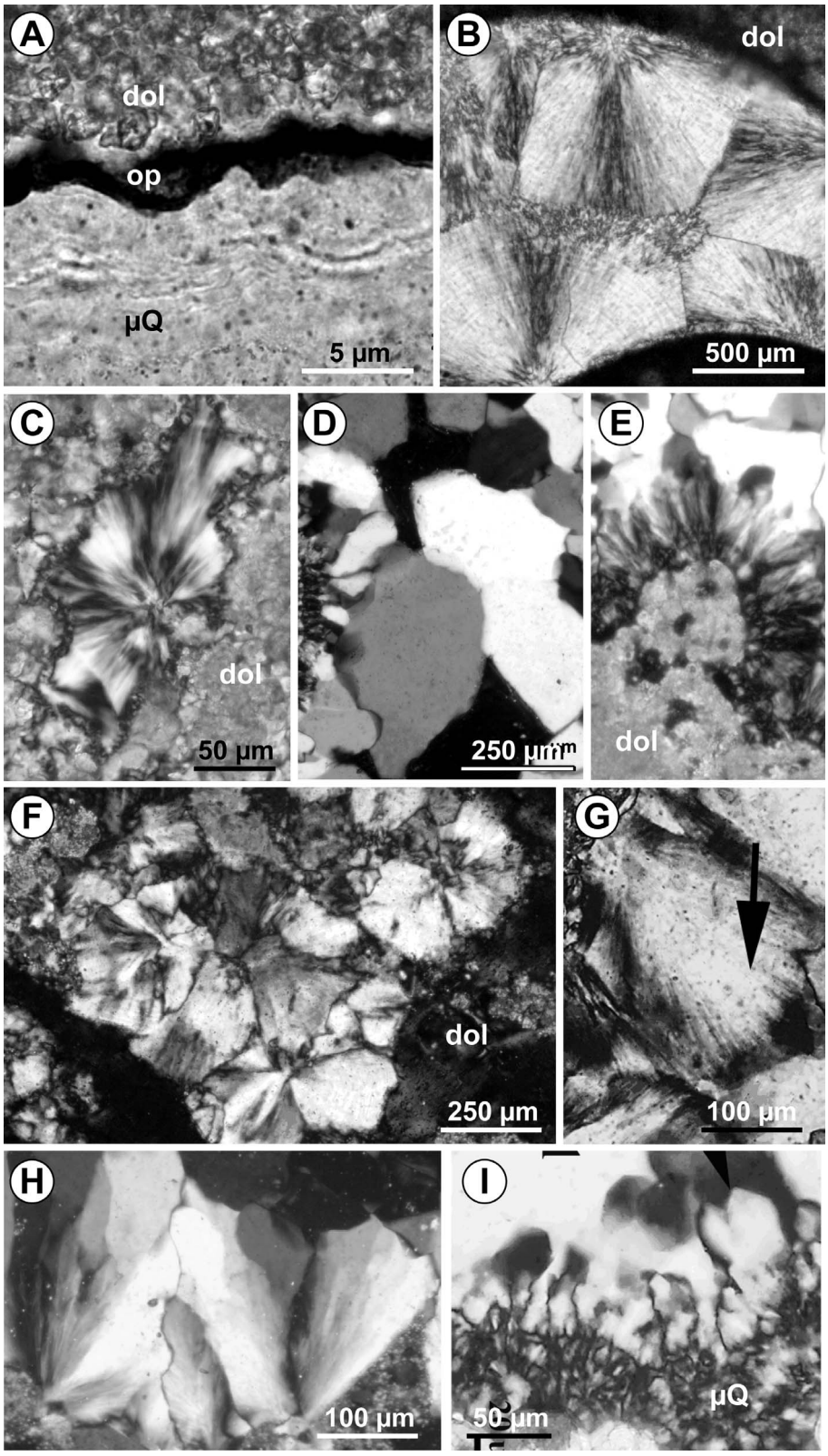

FIG. 5.—Photomicrographs of silica polymorphs. **A)** Brownish laminae of isotropic opal-A (arrow) lining cavity in dolostone infilled with microquartz. **B)** Length-fast banded sheaves of chalcedony. Rectilinear suture lines indicate growth in euhedral fashion. **C)** "Zebraic"- or twisted-chalcedony with variable birefringence along a single fiber. **D)** Equant megaquartz mosaic and palisadic arrangement of smaller megaquartz crystals implanted on cavity wall. **E)** Palisadic quartz crystals with euhedral terminations. **F)** Petaloid of radiant feathery megaquartz crystals with flamboyant extinction. **G)** Megaquartz with feathery extinction. **H)** Elongated prismatic crystals with flamboyant extinction. **I)** Cavity lined with microcrystalline quartz grading to palisadic, elongated flamboyant crystals with euhedral terminations of cubic appearance and uniform extinction. A) plane polarized, B–I) crossed nicols. dol, dolostone; op, opal; µQ, micro-quartz.

chalcedonite sheaves and equant megaquartz have grown directly on the dolostone of the cavity wall (Fig. 6C, D). Megaquartz occurs particularly in the mold cavities that are isolated within the dolostone and away from micro-karst dissolution features.

Matrix Replacement by Silica.—Although silica polymorphs in large voids are relatively easy to identify, this becomes more difficult in smaller pores, especially when laminated deposits or a crystalline sequence is lacking, or when the size of the crystals infilling the pore is comparable to

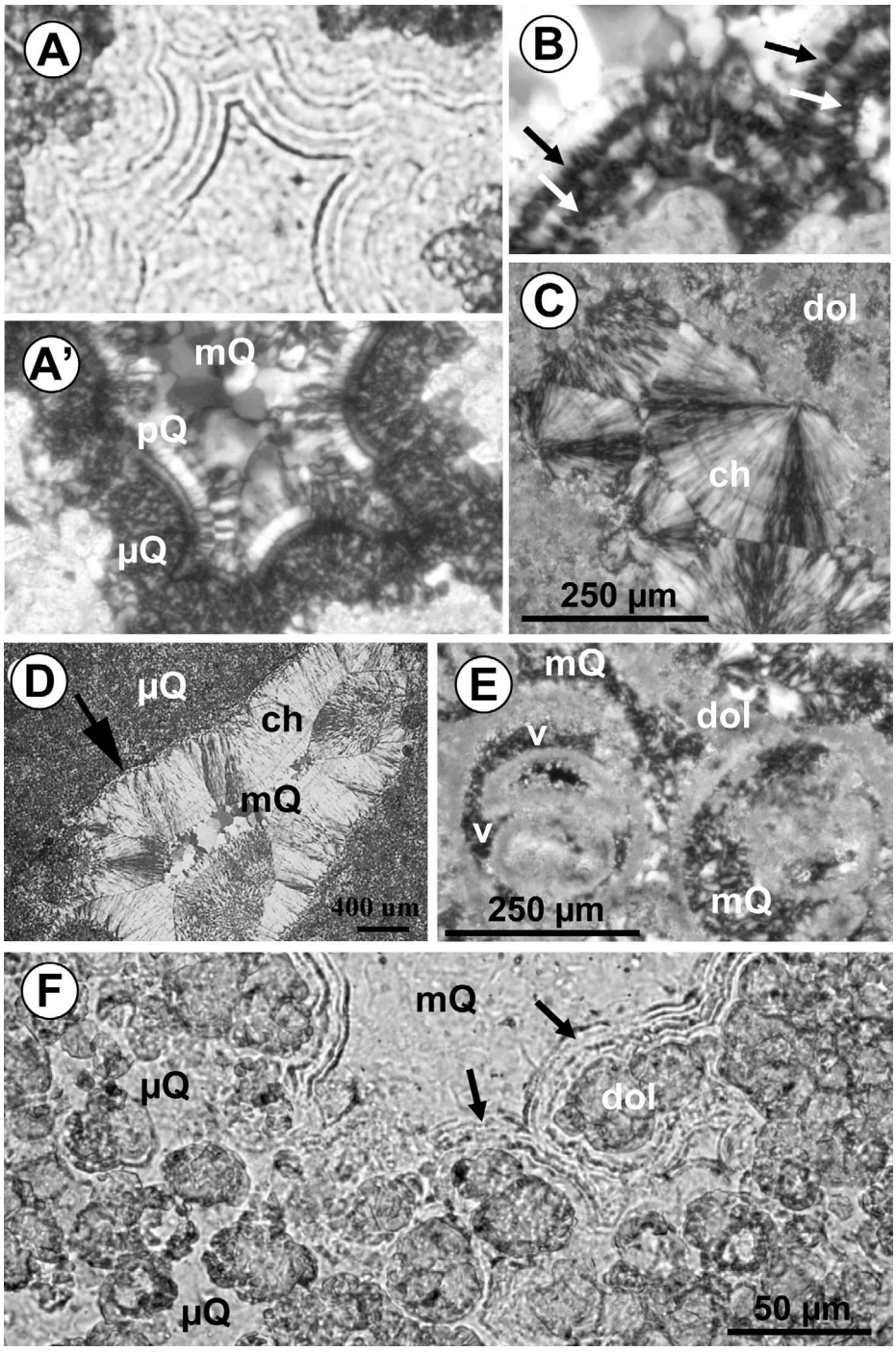

FIG. 6.—Petrography of silica infilled voids. **A)** Silica filling of cavity and **A′)** mirror view of same area with crossed nicols: Roughness of cavity walls smoothed by laminated silica deposits formed of micro- and palisadic quartz. Note central filling of sub-euhedral macroquartz crystals. **B)** Two opal laminae (black and white arrows) within palisadic quartz laminae. **C)** Mammillated chalcedony sheaves with compromise boundary filling cavity. **D)** Cavity infilled by laterally stacked mammillated cones of chalcedony capped by sub-euhedral quartz. **E)** Some intra- and inter-shell cavities filled with radiant megaquartz with flamboyant extinction; others remain empty. **F)** Large dissolution cavity rimmed with laminated silica (arrows) that retract from cavity. Voids are infilled with non-laminated microquartz. A, F) plane polarized, A′–E) crossed nicols. dol, dolostone; μQ, microquartz; pQ, palisadic quartz; mQ, megaquartz; ch, chalcedonite; v, void.

the pore size, with the result that there is only a small number of crystals. It is even more difficult to know if the replacement of dolostone matrix occurred via epigenetic processes, implying that silica precipitation and carbonate dissolution occurred simultaneously. Preservation of primary sedimentary structures (fossils or sparite-filled joints, bioturbation structures, and depositional laminae) within the siliceous matrix, as well as carbonate inclusions in megaquartz, are probably the best criteria to identify epigenetic processes. In the absence of such criteria, epigenetic replacement of the matrix is often assumed by default when pore-infilling structures are lacking. However, in the Dammam Formation dolostones, careful observations at high magnification do in fact reveal microquartz arrangements indicative of void or cavity fillings where microquartz appears to be permeating the dolomitic groundmass (Fig. 7A).

Selective replacement of some carbonate species or structures is another criterion for epigeny. Thereby, selective replacement of dolomicrite groundmass and the preservation of "floating" dolosparite crystals within microquartz seems to be a reliable clue (Fig. 7B). Tiny carbonate inclusions within meso- and megaquartz crystals (Fig. 7C) may be remnants of a primary carbonate matrix and thus evidence of epigenetic replacement, even if the silica and carbonate may also be cogenetic. Thin, clear outer rims of zoned dolomite rhombohedra, characteristic of the hard crystalline dolostone, are in places preserved within a mosaic of

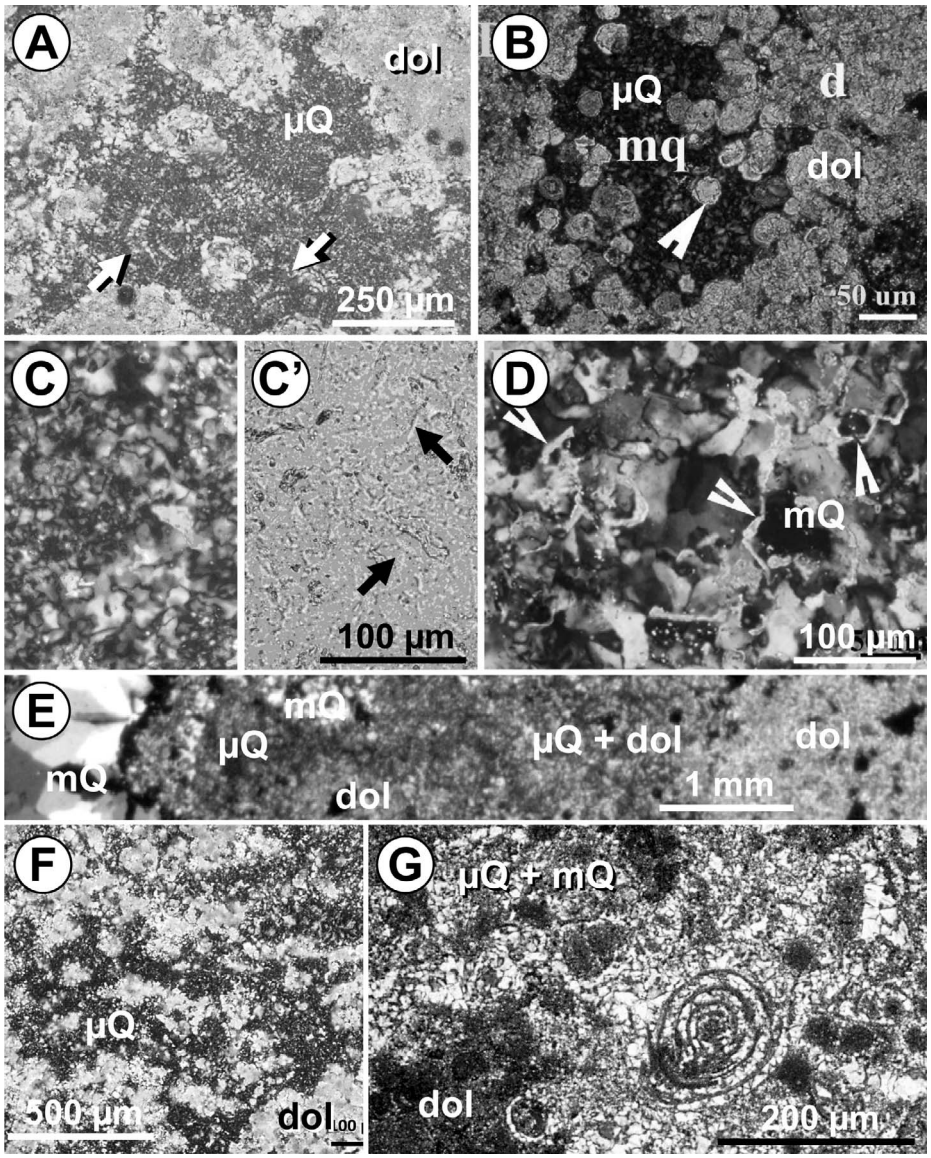

FIG. 7.—Petrography of silica replacing dolostone. **A)** Microquartz seems to be partly replacing dolomitic groundmass. Note alignments of fine quartz (lightly dashed lines shown by arrows) indicating that part of microquartz relates to void filling. **B)** Dolomite rhombs scattered within microquartz mosaic replacing dolomitic groundmass. **C)** Small quartz mosaics with tiny dolomite crystal inclusions shown by arrows in Part C′. **D)** Arrows point to remains of limpid and euhedral dolomite scattered within mosaic of macroquartz crystals. **E)** Cavity filled with megaquartz and connected to irregular, diffuse patches of microquartz replacing dolomitic groundmass fading out away from cavity. **F)** Irregular and diffuse patches of microquartz replacing over 50% of dolostone groundmass. **G)** Whole quartz cement cannot be related to a single dissolution-filling event because residual dolostone structure would have collapsed. Crossed nicols except C′ is plane polarized. µQ, microquartz; mQ, megaquartz; dol, dolostone.

macroquartz crystals (Fig. 7D). The sharpness and the scattered occurrence of these splinters indicates that they are not remnants accumulated in a dissolution cavity. Epigenetic replacement of the primary dolomitic matrix, with selective preservation of the well-crystallized dolomite rims, is the most plausible interpretation of the structures.

It must be emphasized that epigenetic replacements are never completely disconnected from silica-infilled voids. It is around large voids and in zones with numerous cavities that irregular and diffuse microquartz patches occur with transition into mixed silica and dolomite patches away from the voids (Fig. 7E). This points to a spatial relation between silica-infilled voids and epigenetic replacement.

Silicification resulting in extensive indented microquartz patches or even large zones of megaquartz infilling voids, together with microquartz patches containing scattered dolostone remnants (Fig. 7F, G), requires that, in the first case, silicification cannot have resulted from one single void because the rock structure would have collapsed: successive or partial silica replacement is likely to explain these structures. Secondly, there may be progressive dolostone dissolution and concomitant silica deposition in voids along with successive phases of silicification.

Fine Structures of Silica Polymorphs in the Chert.—SEM studies show that the silica polymorphs identified by optical microscopy consist of internal substructures that appear to be rather independent of their optical characteristics.

For example, nanoglobules with smooth surfaces and ranging in size between 0.1 and 0.5 µm constitute the prevailing fabric of most of the studied chert samples. They form heterometric arrays of randomly packed microspheres with neighboring spheres commonly being joined by small connection pads. They may coalesce to form large cauliflower-shaped globules that reach 2 µm in size and frequently form plates with dimensions of several micrometers and with their boundaries well defined (Fig. 8A). Nanoglobules correspond to typical opal-A micromorphologies such as those reported in reference deposits (Segnit et al. 1970; Darragh et al. 1976) and in present-day hot-spring deposits (Herdianita et al. 2000; Rodgers et al. 2004; Lynne et al. 2005).

Fibrous structures formed of well individualized, undulating and wavy interwoven silica fibers (about 100 nm in diameter and up to 10 µm long) occur together with dolomite crystal remnants (Fig. 8B, C). The size of the fibers and their interlaced and crisscrossing arrangements do not match the

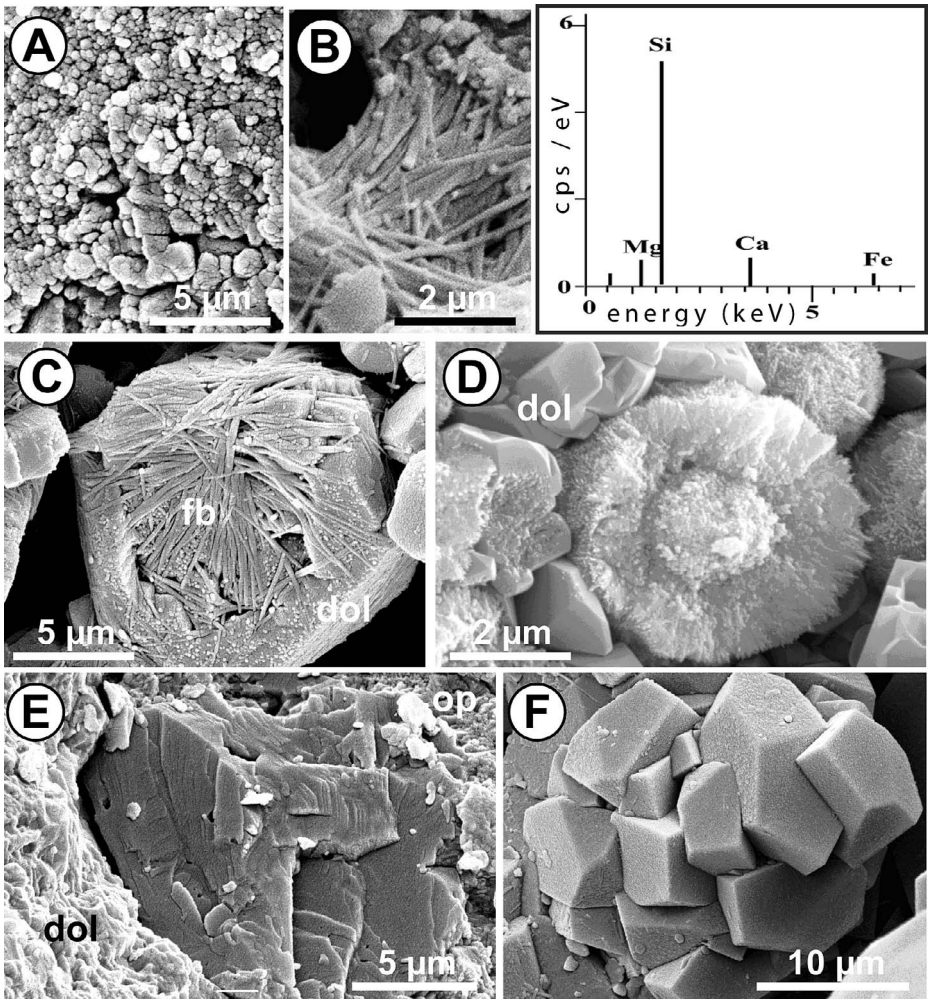

FIG. 8.—Nanofabric of silica polymorphs. **A)** Opal-A nanoglobules. **B)** Interwoven fibers identified by EDS analysis as SiO_2, with traces of Ca and Mg. **C)** Zoned dolomite crystal showing interwoven fibers replacing core while outer limpid zone remains little altered. **D)** Opal-CT lepisphere displaying blade-shaped crystallites consisting of stacked opal-A nanoglobules. **E)** Quartz crystal with conchoidal fracture within dolostone matrix with silica composed of opal nanoglobules. **F)** Jigsaw-textured mosaic of microquartz crystals. SEM analyses. fb, fiber; dol, dolomite; op, opal.

regular parallel fabric of fibrous silica but closely mimic fibrous clay minerals like palygorskite and sepiolite that are commonly associated with dolostones (Singer and Galan 1984; Akbulut and Kadir 2003; Khalaf 2007). Although fibrous clay minerals replacing dolomite can form by addition of silica-rich solutions (Chahi et al. 1999), EDS analyses show that the fibers here are formed almost exclusively of SiO_2, with only traces of Ca and Mg. Fibrous clay minerals can beyond doubt be altered by leaching of cations, leaving residual silica and preserving the mineral fabric, as has been observed for various kinds of clays (Thiry and Milnes 1991; Elsass et al. 2000).

Lepispheres reaching 5 µm in diameter and formed of interpenetrating crystal blades (about 1 µm × 0.1 µm in size) are often present in the chert samples. Some broken lepispheres show internal structures composed of a core up to 1.5 µm in diameter consisting of agglomerated cryptocrystalline silica nanoglobules and a 1-µm-thick rim of radially arranged hexagonal crystal blades (Fig. 8D). Even the crystal blades consist of stacked nanoglobules. This texture should be called paracrystalline, like that of similar materials in hot-spring deposits (Rodgers et al. 2004; Lynne et al. 2005). The arrangement of crystal blades within lepispheres is characteristic of opal-CT (Flörke et al. 1976; Arbey 1980; Thiry and Milnes 1991; Lynne et al. 2005).

Conchoidal fractures are a common feature of silica nodules (Fig. 8E). They are specific to crystal growth by precipitation from solution, which often leads to development of euhedral chalcedonite spherolites or quartz crystals (Fig. 8F).

Recrystallization of Silica Polymorphs in Chert.—SEM observations of chert samples show that the frequency and/or abundance of opal nanoglobules widely exceeds the abundance of opal we recognized using optical microscopy. This means that some of the petrographic varieties of quartz and also of the spherolites and sheaves of chalcedony are in fact formed of nanoglobules. Thus, primary deposits of opal-A have recrystallized into diverse varieties of silica.

Locally, euhedral quartz forms can be seen to emerge from heaps of nanoglobules (Fig. 9A) and appear to develop into drusy quartz crowning agglomerates of nanoglobules (Fig. 9B). The terminal crystal faces of the quartz are smooth surfaces obviously related to growth, whereas the flanks of the crystals display incomplete, rough surfaces of coalesced nanoglobules with a paracrystalline fabric similar to that described in cherts by Hattori et al. (1996). The arrangement of quartz crystals around nanoglobule masses suggests that the center of crystallization of the druse is located within nanoglobules that induced quartz crystal development. Similarly, the common forms of silica infilling voids, namely successive laminae of microquartz lining void walls, overlain by flamboyant palisadic quartz with euhedral terminations (Fig. 6A, A′), as we identified using optical microscopy, are actually deposits of opal-A nanoglobules that later recrystallized to quartz, as shown in SEM studies (Fig. 9C), and are comparable to arrangements described by Herdianita et al. (2000) in modern hot-spring deposits. Crystalline quartz devoid of nanoglobule fabric only appears as euhedral forms of quartz. However, some euhedral megaquartz formed during the ultimate stage of infilling of voids has

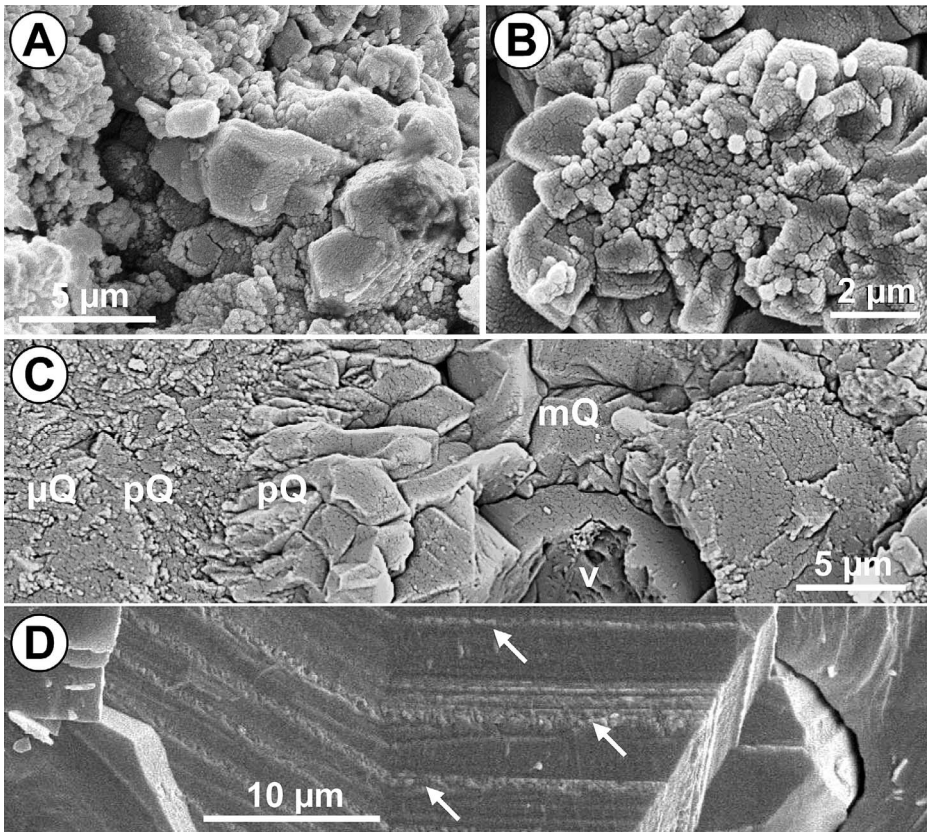

FIG. 9.—Nanofabric of silica deposits. **A)** Smooth surfaces of microquartz crystals emerging from nanoglobule aggregates. **B)** Jigsaw-textured microquartz crystals growing around agglomerate of nanoglobules. **C)** Silica infilling void starts with significant deposits of opal-A nanoglobules prior to growth of quartz. **D)** Fracture across megaquartz showing successive growing bands composed of compact crystal fabric interlayered with tiny nanoglobules (arrows). SEM analyses. µQ, microquartz; pQ, palisadic quartz; mQ, megaquartz; v, vug.

smooth growth steps of compact quartz texture separated by bands of tiny nanoglobules (Fig. 9D).

Continuity of the optical axis between the recrystallized opal nanoglobules and the later quartz crystals, either in the case of flamboyant palisadic quartz with euhedral terminations, or drusy, jigsaw-textured microquartz that emerges from masses of nanoglobules, implies that nanoglobules recrystallized to quartz during the silica precipitation processes, before euhedral quartz growth. Moreover, because the crystallographic continuity of the successive stages of macroquartz growth are not hindered by the interlayered opal deposits, it is concluded that opal recrystallized to quartz immediately after deposition and before the resumption of crystal growth. Comparable features have been described from quartz overgrowths in silicified groundwater sandstones (Thiry and Maréchal 2001) and which turned out to be related to microcrystalline quartz layers within the growth stages (Haddad et al. 2006).

Dating of silica sinter deposits in active hot springs has shown that the change from opal-A to opal C may take place over $\sim$ 50 years and that the onset of quartz crystallization occurs $\sim$ 20,000 years after precipitation of the amorphous silica (Herdianita et al. 2000). In other examples, diagenesis of opal to quartz has been shown in a 1900-year-old siliceous sinter (Lynne et al. 2005). These changes are rapid to extremely rapid in comparison with the geological time scale, even if recrystallization is likely to be facilitated by the warm average ambient temperatures, (around 40–70°C) in hot-spring environments.

Silicification of Dolomite.—The most pervasive texture showing replacement of dolomite by silica consists of indented mosaics of microquartz throughout the dolostone groundmass with, in places, remnants of limpid dolomite rhombs (Fig. 7A, B). SEM images show that replacement of dolomite by silica preserves the nanostructures of dolomite crystals as well as those of paragenetic fibrous clay minerals (Fig. 10A). Moreover, the fibrous clay minerals are leached of cations and dolomite is replaced by opal-A nanoglobules along cleavage planes (Fig. 10B, C). This fine-scale structure points to progressive dissolution of dolomite along cleavage planes and concomitant precipitation of silica: the structure would have collapsed if there had been dissolution of dolomite followed later by precipitation of silica. It is likely that dissolution and precipitation are closely bound reactions: for example, silica precipitation causes dolomite dissolution or, inversely, dolomite dissolution induces silica precipitation. Primary silica in the form of nanoglobules and fibers was opal that later recrystallized to form microquartz. Preservation of primary textures, for example the conservation of connected limpid rims of dolomite rhombohedrons, points to a coupled dissolution–precipitation reaction without formation of dissolution cavities.

In some chert samples, the dolomitic groundmass is replaced by subeuhedral microquartz crystals without any sign of a nanoglobule precursor, and this may have resulted from direct precipitation of quartz from groundwater solution (Fig. 10D).

Finally, along with all of these recrystallization phenomena, there is selective dissolution of some silica, probably the most soluble deposits of opal (Fig. 10E).

DISCUSSION AND CONCLUSIONS

The distribution and fabrics of the Dammam Formation chert, and especially the detailed arrangements of the various silica polymorphs, provide clues about the nature of the silicification processes.

Environment of Silicification

The Dammam Formation dolostones have never been deeply buried, nor have they experienced burial diagenesis under elevated temperatures and pressures. We consider the mineralogical changes in the dolostones, among

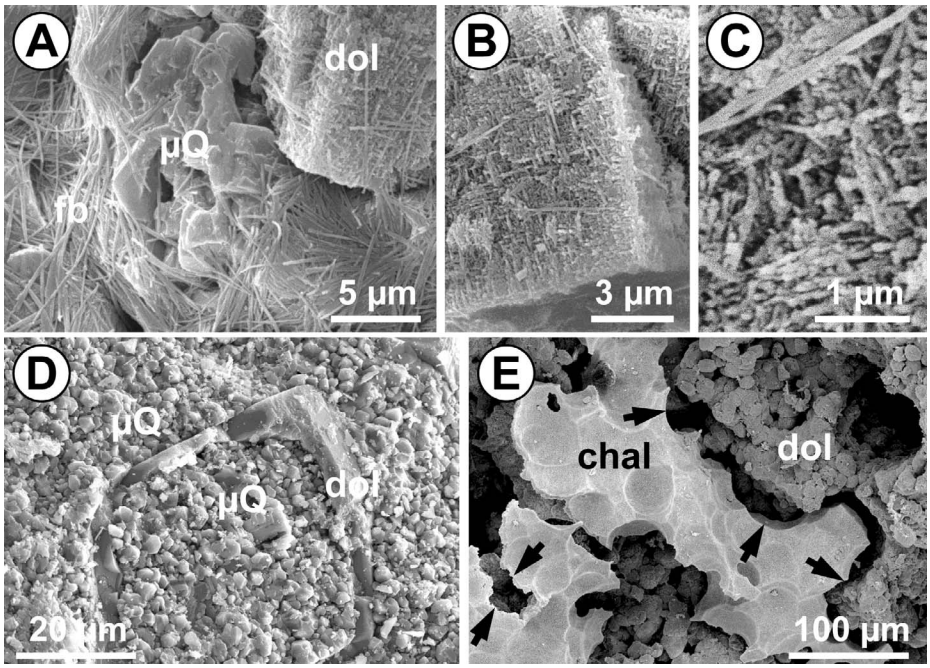

FIG. 10.—Nanofabric of dolomite replacement. **A)** Groundmass of interwoven fibrous clay minerals and rhombohedral dolomite replaced by silica (microquartz in optical microscope). **B)** Dolomite rhombohedron completely replaced by silica. Enlargement in **C)** Silica consists of coalesced stacks of nanoglobules along dolomite cleavage planes. **D)** Arrows point to remains of limpid dolomite zones scattered within mosaic of microquartz crystals. **E)** Chalcedonite spherolites within dolomitic groundmass. Spherolite aggregate is separated from dolomite by bordering void (arrows). SEM analyses. dol, dolomite; fb, fibers; µQ, microquartz; chal, chalcedonite.

them dolomitization, karstification, as well as silicification, to be the result of surface or near-surface processes more or less directly connected to weathering. Based on their disposition as a series of superposed silicified horizons that are in places discordant with bedding, the observation that they are not confined to the more porous primary dolostone layers, and the preservation of primary host-rock structures (stratification, bioturbation, fossils) within them, the Dammam Formation chert layers are interpreted to be a form of groundwater silcrete (Thiry and Milnes 2017).

If our interpretation is correct, each chert horizon is indicative of a particular level of silica precipitation marking the interface between two environments within the groundwater regime, or more probably at the phreatic surface, where specific conditions led to a significant decrease in silica solubility.

Suggested Groundwater Regime and the Origin of the Silica

Because there is no significant source of silica in the dolostones, it has to be imported from other sources and brought into the horizon where chert formation occurred. The relatively low solubility of silica in surficial waters and the large volume of silica needed to effect silicification imply that significant volumes of silica-bearing solutions flowed through the dolostone to fulfill the mass balance. This requires a groundwater head and a groundwater outflow zone (springs, seeps) and implies landscape incision in order to intersect the groundwater system. Similarly, micro-karstic dissolutions of the dolostones that generate porosity into which incoming silica was precipitated can occur only via water flows.

Sourcing the silica is not a crucial problem. There is always silica available for solution in sedimentary formations, from the dissolution of silica minerals present and/or the alteration of silicate minerals, in particular clay minerals. Globally, most groundwaters have a silica content between 12 and 20 mg/L SiO_2 (White et al. 1963; Davies 1964; Garrels and Christ 1965; Hem 1985) that is roughly in equilibrium with clay minerals. This means that most groundwaters are supersaturated with respect to quartz (solubility 4–7 mg/L) and thus may be able to precipitate quartz if physicochemical conditions are favorable.

The silica forming the Dammam Formation chert could have been sourced either directly from the alteration of clay mineral components of the dolostones, or from a siliciclastic cover over the Dammam Formation before deposition of the Kuwait Group, or even from more distant regions as far away as the Arabian Shield or the Zachros Fold Belt, according to tectonic and eustatic conditions at the time (Al-Sulaimi and Al-Ruwaih 2004). Only weak alteration or weathering of large volumes of rocks at a regional scale is sufficient to source the silica required (Thiry et al. 1988).

Silica Precipitation

Precipitation of silica is the mainspring of silicification: understanding it is the key to understanding the system. Silica in solution in water imported to the formation is precipitated when its solubility is lowered. Many geochemical processes have been proposed to explain silicification or, more precisely, silica supersaturation and precipitation. For example:

- **Concentration of silica** in solution may be increased sufficiently by evaporation for silica to precipitate. This can happen only at the landsurface and does not generate superimposed horizons of silicification that have sharp contacts with the host formation (Thiry and Milnes 2017).
- **Redox** reactions have no direct effect on silica solubility: silica may combine with organic compounds to form organo-silica complexes that enhance the solubility of silica (Bennett 1991), with microorganisms possibly also contributing (Ewans 1964). On the other hand, to our knowledge, no study has pointed to silica precipitation being facilitated by organic compounds.
- **pH reduction** is not a widespread mechanism for silica precipitation in natural environments, contrary to what is often suggested. Effectively, the solubility of silica in water is steady until pH 8.5 and increases significantly above pH 9 (Krauskopf 1956; Siffert 1967). So, by lowering the pH of an alkaline solution saturated in silica, some of the silica in solution will precipitate. However, such high pH values are rare in natural environments, and are restricted mainly to alkaline evaporitic environments with Na-carbonate–bicarbonate brines (Eugster and Hardie 1978). These alkaline conditions are not relevant to groundwater silicification. Even if alkaline brines exist in groundwaters, they will be limited to evaporitic and endorheic basins that essentially have no outflow and thus are not able to provide the large volumes of water

needed to provide the necessary silica for silicification in supergene environments.

- **Increasing salt concentrations** in solution decreases the solubility of silica, in the case of amorphous silica by up to 96% in a saturated solution of $CaCl_2$ and by up to 30% in saturated solution of NaCl (Marshall and Warakomski 1980). So, the mixing of a silica solution with chlorite- or sulfate-rich brine may induce silica precipitation. However, the difficulty in promoting this mechanism is to propose how waters of very contrasting density could mix and also how the nourishing waters would not be diluted during the mixing. Nevertheless, silica precipitation via salinization is likely to have been a mechanism involved in the formation of groundwater silcretes (jasper and porcelanite) in inland Australia where there are associated sulfates (mainly gypsum, alunite,,,, and jarosite) (Thiry et al. 2006). In the case of the Dammam Formation chert there is no evidence for evaporite minerals in the host sediments or in the chert.
- **Lowering temperature** acts in a very significant way on the solubility of silica (Williams et al. 1985; Rimstidt 1997). The mechanism has been advocated in deep hydrothermal environments (Fournier 1985; Hendry and Trewin 1995) and is clearly shown in hot-spring systems (e.g., Renaut and Owen 1992; Guidry and Chafetz 2002), but it has not been envisaged as a factor in precipitating silica in the supergene realm. Indeed, the solubility of quartz decreases with temperature according to an exponential law: it is more than halved by cooling the solution from 25°C to 12.5°C (Thiry and Milnes 2017). This would appear to be a very efficient mechanism for precipitating silica from solution as has recently been shown by Thiry et al. (2015a, 2015b). During cold periods silica dissolved in groundwater may thus precipitate if the water cools significantly by moving closer to the land surface.

We suggest that groundwater cooling is the most likely process to account for silica precipitation to form the chert horizons in the Dammam Formation dolostones, with chert layers corresponding to various positions of the phreatic surface of the groundwater. The superimposed chert horizons may correspond to successive falls of the phreatic surface caused by landscape incision, with the oldest at the top of the sequence (corresponding to the initial position of the phreatic surface and the youngest at the base, similarly to that documented within the Tertiary sandstones in the Paris Basin (Thiry et al. 1988, 2015a). This systematic arrangement of chert horizons is indicated by a lack of overprinting features in the chert layers, which would have occurred if the groundwater level was fluctuating through time. The greater degree of silicification of the dolostone (number and volume of masses in the chert horizons) higher in the section could potentially be related to a sharper cold front near the paleosurface at time of initial silicification, and thus a more efficient silica precipitation process. A lower degree of silicification at depth in the section could record a temperature gradient away from the cold front, combined with a gradual disruption of the groundwater source and flow regime as landscape incision progressed.

Water Geochemistry

Silica polymorphs reflect the chemistry of the solution from which they precipitated. The formation of amorphous silica requires solutions with high degrees of silica supersaturation with some degrees of polymerization promoting the formation of abundant nuclei with a high growth rate (Iler 1979; Fournier 1985; William and Crerar 1985). On the other hand, solutions that are less supersaturated with silica and have a limited number of nuclei favor the precipitation of large quartz crystals with a slow growth rate (Delmas et al. 1982; Williams and Crerar 1985). Indeed, the degree of supersaturation is more relevant than the concentration of the solution itself. The degree of supersaturation results from a discrepancy between rates of silica precipitation and growth of silica polymorphs. High degrees of supersaturation indicate large and rapid, even abrupt, changes in the physicochemical properties of the solution, whereas low degrees of supersaturation, or even equilibrium of the solution with a mineral species, result from more subtle and progressive changes in physicochemical characteristics of the solution. The formation of opal indicates a strong gradient in a physicochemical agent which causes silica to precipitate, namely between the sourcing solution and the host rock, whereas the crystal growth of megaquartz points to some form of mitigation of the physicochemical imbalance between the solution and the host rock.

Carbonate replacement by silica is another aspect that may help to define some geochemical constraints. In the case of the Dammam Formation chert, dolomite replacement by silica proceeds volume-for-volume and carbonate dissolution is restricted to silica–carbonate contacts. We assume that silica precipitation and dolomite dissolution occurred simultaneously and thus the pressure of quartz crystallizing against dolomite may have induced dissolution of the latter (Maliva and Siever 1988b, Minguez and Elorza 1994). That dolomite has not reprecipitated near the pressure points means that the pervading groundwater solution was weakly undersaturated with regard to dolomite. There may also have been a feedback from cooling of the groundwater solution. In the first instance, the groundwater would have been in equilibrium with dolomite. Its CO_2 fugacity would have increased as it cooled down in contacting the host rock and thereby it would have become undersaturated with respect to dolomite. The concomitant development of microkarstic cavities and their infilling with silica in the dolostones appears to have resulted from this sort of coupling effect.

Sulfate and carbonate anions appear to have a specific influence on quartz crystallization. For a long time it has been argued that length-slow chalcedony crystallizes preferentially in the presence of sulfates whereas carbonate anions favor the development of length-fast chalcedony (Folk and Pittman 1971; Arbey 1980, Khalaf 1988). In the Dammam Formation chert, length-slow silica pseudomorphs (length-slow chalcedony, twisted chalcedony, flamboyant palisadic quartz and feathery quartz) are common and occur mainly in the silica laminae lining cavity walls. Length-fast chalcedony occurs in the central parts of void infillings or directly on the walls of fossil mold voids that are devoid of laminated silica deposits. That length-slow and length-fast species succeed each other in the depositional sequence of silica infillings points to a chemical evolution of the solution. Initially, the presence of SO_4 anions inherited from syngenetic dolomitization of the sedimentary sequence within mixed-zone environments would have influenced the development of length-slow silica polymorphs, but as the inherited SO_4 anions were leached by groundwater flow-through the crystallization of length-fast chalcedony was favored.

Recrystallization Processes

In the Dammam Formation chert, recrystallization of silica has accompanied several morphological changes of nano- and micro-textures, particularly as opal-A crystallized to paracrystalline opal-CT, which then recrystallized to chalcedony, and micro- meso-, and megaquartz with flamboyant or feathery textures. In the first instance, non-crystalline opal-A, commonly deposited as nanoglobules, transformed in stepwise fashion to more thermodynamically stable phases (aging or maturation). Willey (1980) showed that recrystallization of silica is accompanied by a decrease in solubility of about 20% and a decrease of specific surface area of about 50%. In addition, Williams et al. (1985) stated that the relationship between solubility and surface area or particle size is sufficient to explain transformations of opal-A to opal-CT to quartz.

Silica remained mobile throughout ongoing silicification and/or post-silicification transformations in the Dammam Formation chert, resulting in a wide range of silica pseudomorphs. The dissolution and deposition of the silica forms were driven by the differing solubilities of the successive phases. At each stage of maturation, a less-mature phase was dissolved,

transported via diffusion, and precipitated as a more mature phase, as was shown by dissolution nanostructures associated with crystallization of new species (Rodgers et al. 2004; Lynne et al. 2005). The process was sustained by silica migration through a network of sources and sinks, with sources consisting of the inherited more soluble phases and sinks corresponding to the sites where more stable phases of lower solubility crystallize. This process probably operated at heterogeneous macroscopic or microscopic scales within the chert masses.

Transfers of silica operated at a nano-scale and did not involve chemical exchanges or migrations at a macroscopic scale with the host rock. Accordingly, the chemical differentiations which may have existed between successive deposits of nanoglobule laminae on void walls may actually have persisted through all these transformations and could be reflected in the recrystallized mineral phases. This explains why, after the final stage of recrystallization, the successive laminae of opal-A nanoglobules are still recognized in the differentiation of the quartz polymorphs to which they gave birth and in some interstratified laminae have not recrystallized.

Mineralogical Succession of Silica Deposits

All silica infillings in voids show similar mineral successions that are initially cryptocrystalline (amorphous) forms of opal and subsequently better developed crystals of chalcedony (sheaves) and microquartz and, ultimately, euhedral quartz. Such sequences were described in the first petrographical studies, over a century ago, in numerous sedimentary sequences as well as in hydrothermal veins (Cayeux 1897; Storz 1926; Hendry and Trewin 1995). This succession is systemic: reverse or recurrent sequences are never observed, which points to precipitation from a progressively diluting solution of silica, or rather to a decrease of the degree of supersaturation of the solution. The initial deposits would have formed from highly supersaturated solutions generating high precipitation rates inclusive of impurities and foreign cations. The later deposits would have developed from more diluted and only slightly oversaturated solutions that induced a slow growth of purer quartz crystals (Milliken 1979; William and Crerar 1985; Thiry and Millot 1987; Heaney 1993).

The compositional changes in the solutions that are indicated by the observed succession of silica precipitates are somehow self-organized in response to the progressive silicification of the host rock. Initially, the incoming solutions were likely to have induced some alteration or dissolution of the Dammam Formation dolostones. We suggest that supersaturation in silica became enhanced by a relatively strong temperature gradient between warmer groundwater and host dolostone in a cold regolith environment predating karst formation (and the deposition of the Kuwait Group sediments), and this led to rapid precipitation of poorly crystallized silica polymorphs. As silicification progressed, the pervading groundwater solution became progressively insulated from the host rock by the newly formed silica deposits and thus became less mineralized by dissolution of the Dammam Formation dolostones. At the same time, the temperature gradient may have been lowered by warming of the dolostones by groundwater flowing through them. Ultimately, there was slow precipitation of better-crystallized silica species. The final silica phases would have been precipitated from solutions largely unaffected by the host rock, and thus reflect the intrinsic geochemical characteristics of the sourcing solution. When chalcedony and quartz crystallized in voids, the parent solution was relatively dilute fresh water containing only low concentrations of cations other than Si.

Suggested Model for Silicification

The chert of the dolostone sequence is characterized by: 1) arrangement in extended layers that are somewhat disconformable to bedding and have sharp boundaries with the host rock; 2) a tight structure resulting from silica infilling voids and replacing dolostone matrix; and 3) a composition composed of a specific succession of mineralogical forms of silica terminating in the precipitation of quartz crystals. These features define the characteristics of the solutions that generated silicification, which can be summarized as follows: 1) silica was imported into the zones of silicification because the dolostone does not contain a significant silica source (neither biogenic nor mineral); 2) large quantities of water were necessary to import the silica; 3) a change of physicochemical characteristics in the environment was necessary to cause silica precipitation; and 4) the accumulation of large amounts of opal in each horizon indicates that the silica precipitated from highly supersaturated silica solutions at an interface where there was likely to be a very strong physicochemical gradient.

The regularity and the planar form of each of the chert horizons points to a precipitation interface that was relatively stable for a time, and we suggest that this corresponded to the phreatic surface of local or regional groundwater. Of many physicochemical conditions that could have induced silica precipitation from groundwater, we suggest that the most likely to have maintained high and long-standing oversaturation along a stable surface was a decrease in temperature.

The field characteristics and petrography of the chert in the Dammam Formation dolostones are very similar to that of groundwater silcretes described elsewhere in quite different geological settings. These forms of silicification reflect significant water flows that provided the silica and substantial landscape relief that provided a hydraulic gradient that drove water flows, and our studies of these silcretes have provided the basis for a model for the formation of the Dammam Formation dolostone cherts, as shown schematically in Figure 11.

The timing of chert formation is clear from field relations: it has to predate the development of karst in the dolostones (because chert horizons are much disrupted and eroded during karst formation), and thereby predate the deposition of Mio-Pleistocene Kuwait Group sediments that unconformably overlie the Dammam Formation and infill the karst landscape. Groundwater flowing according to the hydraulic regime from highland to local or regional discharge areas (which may have been controlled locally by landscape incision) intersected a cold near-surface zone. (Fig. 11A, B). This generated the physicochemical changes that we suggest led to silica precipitation and concomitant accompanying alterations (Fig. 11C), namely: 1) a reduction in temperature of the groundwater solution; 2) a decrease in silica solubility and supersaturation of the solution; 3) a slight increase in aqueous CO_2 and a correlative decrease in pH, which gave rise to microkarstic dissolution of dolomite; and 4) the precipitation of a specific sequence of silica forms in response to progressive cooling of the groundwater solution and the correlative increase in oversaturation.

In generating the proposed model, we have considered the following:

- Because we believe that cooling of the incoming groundwater is connected to the landsurface, we would expect that there was a sharp near-surface temperature boundary and a gradient in temperature with depth. Amorphous silica precipitated against the cold front where supersaturation was greatest, and this formed the initial silica cement in the host rock. Downstream, the groundwater was exhausted in silica, and it was no longer precipitated. Upstream, on the other hand, there was only limited supersaturation that could generate crystal precipitates over previously formed opal-A.
- A slight pH decrease at the cold front triggered some microkarstic dissolution of the dolostone matrix. This additional porosity maintained groundwater flow and further silica precipitation that helped to achieve dolomite replacement by silica. Leaching of dolomite re-equilibrated the solution, and microkarstic dissolution did not continue downstream. Even if dolostone dissolution and silica precipitation are bound to the same temperature drop, dolomite dissolution seems to have preceded

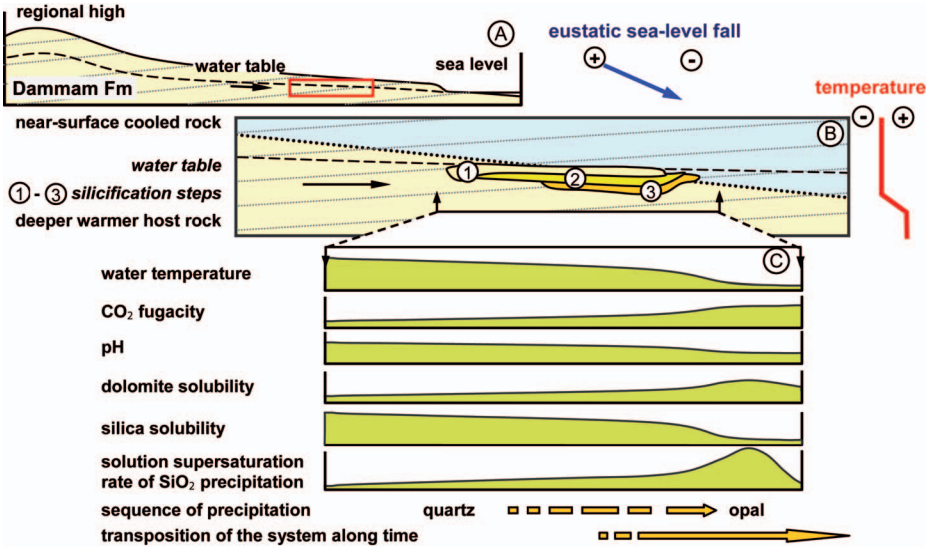

FIG. 11.—Conceptual model of hydrological and thermal arrangements within the Dammam Formation during cold-climate event. Interface between cold subsurface (vadose zone) and warmer groundwater (phreatic zone) facilitated concomitant microkarstic dissolution of host dolostone matrix and precipitation of silica. Progressive warming of host rock via groundwater flow transferred the reactive front downstream. Several self-organizational processes explain numerous field and petrographic characteristics of the chert layers.

silica precipitation because the dolomite dissolution rate was higher than the rate of silica precipitation.

- The formation of a chert layer is unlikely to have been generated in a single step, even if dissolution of the dolostone matrix occurred throughout the silicification process. A progressive reduction in porosity would probably have caused the flow of groundwater to bypass the partially silicified zone and complete replacement of the dolostone would not have occurred. We suggest that silicification proceeded by means of successive aggradations of silica deposits (Fig. 11B) to generate thick, tight, and uniform silicified masses, as has been described for silicified sandstone bodies (Thiry and Maréchal 2001).
- The superimposed chert horizons most probably correspond to a systematic fall in the groundwater table related to progressive landscape incision (Fig. 11A). Irregular changes in groundwater levels according to geodynamics, climate, and eustatic sea-level changes cannot be excluded, although there is no evidence of "overprinting" within the silicified horizons.

Dating Chert Formation

We have no definitive data on which or whether any of several global cooling events identified in the time period (around 50 Myr) between the deposition of the Dammam Formation (Eocene) and the unconformably overlying Kuwait Group (Mio-Pleistocene) could have accounted for the cold regolith conditions we have proposed for the environment of formation of the Dammam Formation chert. For example, there was a glaciation during the early Oligocene, approximately 33.7 Myr ago, with ice sheets about 25% larger than present, relative sea level about 67 m lower (Katz et al. 2008) and a 5°C lower sea surface temperature at high latitude (45° to 70°) (Zachos et al. 2001a; Liu et al. 2009). A second glaciation has been recorded at the Oligocene–Miocene boundary about 23 Myr ago (Zachos et al. 2001b), with an ice volume between 50% and 125% of the present-day Antarctic ice sheet, and bottom-water temperatures were between ~ 1 and 2°C (Pekar and DeConto 2006; Liebrand et al. 2011). A third, less intense glaciation has been recorded during the Miocene, around 14 Myr, with the Antarctic ice volume estimated to be about 25–70% of that at present (Holbourn et al. 2005; Pekar and DeConto 2006).

Even if regolith cooling was not as substantial as in more northern regions, the Arabian Gulf area was likely to have been affected by these global cooling events. If we assume that the average surface temperature was lowered by 5°C, that groundwater temperature remained at 20°C, and that permeable near-surface formations cooled down to 15°C, the solubility of quartz in groundwater coming into contact with these regolith conditions would have been lowered significantly from 5.5 to 4 ppm SiO_2, that is, about 25%. If the temperature differential was lower, then there would have to have been more water flowing through the Dammam Formation dolostones to precipitate a given amount of silica: that is, more time at a given flow rate. In the Paris Basin, well-dated quartzitic sandstone pans relating to Quaternary glacial periods may have formed in a few tens of thousands of years (Thiry et al. 1988, 2015a).

ACKNOWLEDGMENTS

The authors acknowledge with deep appreciation the support of the General Science Facility (GS01/01) and the Nanoscopy Unit of the Faculty of Science at Kuwait University for providing analytical services. Special thanks are due to Mr. Nabil Basili, Mr. Yousef Abdullah, and Mr. Hisham Mahmoud for their assistance with the field and laboratory work.

REFERENCES

AL-AWADI, E., MUKHOPADHYAY, A., AND AL-SENAFY, M.N., 1998, Geology and hydrogeology of the Dammam Formation in Kuwait: Hydrogeology Journal, v. 6, p. 302–314.

ALEXANDRE, A., MEUNIER, J.-D., LLORENS, E., HILL, S.M., AND SAVIN, S.M., 2004, Methodological improvements for investigating silcrete formation: petrology, FT-IR and oxygen isotope ratio of silcrete quartz cement, Lake Eyre Basin (Australia): Chemical Geology, v. 211, p. 261–274.

ALIMEN, H., 1936, Étude sur le Stampien du Bassin de Paris: Société Géologique de France, Mémoires, v. 31, 309 p.

ALIMEN, H., AND DEICHA, G., 1959, Observations pétrographiques sur les meulières pliocènes: Société Géologique de France, Bulletin, série 6, v. 8, p. 77–90.

AKBULUT, A., AND KADIR, S., 2003, The geology and origin of sepiolite, palygorskite and saponite in Neogene lacustrine sediments of the Serinhisar–Acipayam Basin, Denizli, SW Turkey: Clays and Clay Minerals, v. 51, p. 279–292.

AL-SULAIMI, J.S., AND AL-RUWAIH, F.M., 2004, Geological, structural and geochemical aspects of the main aquifer systems in Kuwait: Kuwait Journal of Science and Engineering, v. 31, p. 149–174.

ARAKEL, A.V., JACOBSON, G., SALEHI, M., AND HILL, C.M., 1989, Silicification of calcrete in paleodrainage basins of the Australian arid zone: Australian Journal of Earth Sciences, v. 36, p. 73–89.

ARBEY, F., 1980, Les formes de la silice et l'identification des évaporites dans les formations silicifiées: Centres de Recherches Exploration-Production Elf-Aquitaine, Bulletin, v. 4, p. 309–365.

BANKS, N.G., 1970, Nature and origin of early and late cherts in the Leadville Limestone, Colorado: Geological Society of America, Bulletin, v. 81, p. 3033–3048.

BENNETT, P.C., 1991, Quartz dissolution in organic-rich aqueous systems: Geochimica et Cosmochimica Acta, v. 55, p. 1782–1797.

BIGGS, D.L., 1957, Petrography and Origin of Illinois Nodular Cherts: Urbana, Illinois State Geological Survey, Circular 245, 25 p.

Burdon, D.J., and Al-Sharhan, A., 1968, The problem of the palaeokarstic Dammam limestone aquifer in Kuwait: Journal of Hydrology, v. 6, p. 385–404.
Cayeux, L., 1897, Contribution à l'étude micrographique des terrains sédimentaires. I. Étude de quelques dépôts siliceux secondaires et tertiaires du bassin de Paris et de la Belgique. II. Craie du bassin de Paris: Lille, Société Géologique du Nord, Mémoire, v. IV/2, 589 p.
Cayeux, L., 1929, Les roches sédimentaires de la France. Roches siliceuses: Mémoires pour Servir à L'explication de la Carte Géologique Détaillée de la France, 774 p.
Chahi, A., Duringer, P., Ais, M., Bouabdelli, M., Gauthier-Lafaye, F., and Fritz, B., 1999, Diagenetic transformation of dolomite into stevensite in lacustrine sediments from Jbel Rhassoul, Morocco: Journal of Sedimentary Research, v. 69, p. 1123–1135.
Chowns, T.M., and Elkins, J.E., 1974, The origin of quartz geodes and cauliflower cherts through silicification of anhydrite nodules: Journal of Sedimentary Petrology, v. 44, p. 885–903.
Daley, B., 1989, Silica pseudomorphs from the Bembridge limestone (upper Eocene) of the Isle of Wight, southern England and their palaeoclimatic significance: Palaeogeography, Palaeoclimatology, Palaeoecology, v. 69, p. 233–240.
Darragh, P.J., Gaskin, A.J., and Sanders, J.V., 1976, Opals: Scientific American, v. 234, p. 84–94.
Davies, S.N., 1964, Silica in streams and groundwater: American Journal of Science, v. 262, p. 870–890.
Delmas, A.B., Garcia-Hernandez, J.E., and Pedro, G., 1982, Discussion sur les conditions et les mécanismes de la formation du quartz à 25° C en milieu ouvert. Analyse réactionelle par voie cinétique: Sciences Géologiques Bulletin, v. 35, p. 81–91
Elsass, F., Dubroeucq, D., and Thiry, M., 2000, Diagenesis of silica minerals from clay minerals in volcanic soils of Mexico: Clay Minerals, v. 35, p. 477–489.
Eugster, H.P., and Hardie, L.A., 1978, Saline lakes, *in* Lerman, A., ed., Lakes: Chemistry, Geology, Physics: Springer Verlag, p. 237–293.
Ewans, W.D., 1964, The organic solubilization of minerals in sediments, *in* Colombo, U., and Hobson G.B., eds., Advances in Organic Geochemistry: New York, MacMillan, p. 263–270.
Fersmann, A., and Wlodawetz, N., 1926, Über die Erscheinung der Silizierung in der Mittelasiatischen Wüste Karakum: Académie des Sciences de l'URSS, Comptes Rendus, p. 145–148.
Flörke, O.W., Hollmann, R., Von Rad, U., and Rosch, H., 1976, Intergrowth and twinning in opal CT lepispheres: Contributions to Mineralogy and Petrology, v. 58, p. 235–242.
Folk, R.L., and Pittman, J.S., 1971, Length-slow chalcedony: a new testament for vanished evaporites: Journal of Sedimentary Petrology, v. 41, p. 1045–1058.
Fournier, R.O., 1985, The behavior of silica in hydrothermal solutions: Reviews in Economic Geology, v. 2, p. 45–60.
Fuchs, W., Gattinger, T.E., and Holzer, H.F., 1968, Explanatory text to the synoptic geology map of Kuwait: Geological Survey of Austria, Vienna, 87 p.
Garrels, R.M., and Christ, C.L., 1965, Solutions, Minerals, and Equilibria: New York, Harper and Row, 450 p.
Guidry, S.A., and Chafetz, H.S., 2002, Factors governing subaqueous siliceous inter precipitation in hot springs: examples from Yellowstone National Park, USA: Sedimentology, v. 49, p. 1253–1267.
Haddad, S.C., Worden, R.H., Prior, D.J., and Smalley, P.C., 2006, Quartz cement in the Fontainebleau Sandstone, Paris Basin, France: crystallography and implications for mechanisms of cement growth: Journal of Sedimentary Research, v. 76, p. 244–256.
Hattori, I., Umeda, M., Nakagawa, T., and Yamamoto, H., 1996, From chalcedonic chert to quartz chert: diagenesis of chert hosted in a Miocene volcanic–sedimentary succession, central Japan: Journal of Sedimentary Research, v. 66, p. 163–174.
Heaney, P.J., 1993, A proposed mechanism for the growth of chalcedony: Contributions to Mineralogy and Petrology, v. 11, p. 66–74.
Hem, J.D., 1985, Study and interpretation of chemical characteristics of natural water, Third Edition: U.S. Geological Survey, Water-Supply Paper 2254, 263 p.
Hendry, J.P., and Trewin, N.H., 1995, Authigenic quartz microfabrics in Cretaceous turbidites: evidence for silica transformation processes in sandstones: Journal of Sedimentary Research, v. 65, p. 380–459.
Herdianita, H.R., Browne, P.R.L., Rodgers, K.A., and Campbell, K.A., 2000, Mineralogical and textural changes accompanying ageing of silica sinter: Mineralium Deposita, v. 5, p. 48–62.
Holbourn, A., Kuhnt, W., Schulz, M., and Erlenkeuser, H., 2005, Impacts of orbital forcing and atmospheric carbon dioxide on Miocene ice-sheet expansion: Nature, v. 438, p. 483.
Iler, R.K., 1979, The Chemistry of Silica: Solubility, Polymérisation, Colloid and Surface Properties and Biochemistry: New York, John Wiley and sons, 866 p.
Kaiser, E., 1928, Die chemische Gesteinsaufbereitung in der Südlichen Namib, *in* Kaiser E., ed., Die Diamantenwüste Sudwestafrikas: Berlin, Dietrich Reiner, sect. 26, p. 283–316.
Katz, M.E., Miller, K.G., Wright, J.D., Wade, B.S., Browning, J.V., Cramer, B.S., and Rosenthal, Y., 2008, Stepwise transition from the Eocene greenhouse to the Oligocene icehouse: Nature Geoscience, v. 1, p. 329.
Khalaf, F.I., 1988, Petrography and diagenesis of silcrete from Kuwait: Arabian Gulf: Journal of Sedimentary Petrology, v. 58, p. 1014–1022.
Khalaf, F.I., 2007, Occurrences and genesis of calcrete and dolocrete in the Mio-Pleistocene fluviatile sequence in Kuwait, northeast Arabian Peninsula: Sedimentary Geology, v. 199, p. 129–139.
Khalaf, F.I., Mukhopadhyay, A., Naji, M., Sayed, M., Shublaq, W., Al-Otaibi, M., Hadi, K., Siwek, Z., and Saleh, N., 1989, Geological assessment of the Eocene and Post-Eocene aquifers of Umm Gudair, Kuwait: Kuwait Institute for Scientific Research, Report No. EES-91- KISR3176.
Khalaf, F.I., Abdullah, F.A., and Gharib, I.M., 2018, Petrography, diagenesis and isotope geochemistry of dolostones and dolocretes in the Eocene Dammam Formation, Kuwait: Arabian Gulf: Carbonates and Evaporites, v. 33, p. 87–105.
Krauskopf, K.B., 1956, Dissolution and precipitation of silica at low temperature: Geochimica et Cosmochimica Acta, v. 10, p. 1–27.
Liebrand, D., Lourens, L.J., Hodell, D.A., De Boer, B., Van de Wal, R.S.W., and Pälike, H., 2011, Antarctic ice sheet and oceanographic response to eccentricity forcing during the early Miocene: Climate of the Past, v. 7, p. 869–880.
Liu, Z., Pagani, M., Zinniker, D., DeConto, R., Huber, M., Brinkhuis, H., Shah, S.R., Leckie, R.M., and Pearson, A., 2009, Global cooling during the Eocene–Oligocene climate transition: Science, v. 323, p. 1187–1190.
Lynne, B.Y., Campbell, K.A., Moore, J.N., and Browne, P.R.L., 2005, Diagenesis of 1900-year-old siliceous sinter (opal-A to quartz) at Opal Mound, Roosevelt Hot Springs, Utah, USA: Sedimentary Geology, v. 179, p. 249–278.
Maliva, R.G., and Siever, R., 1988a, Pre-Cenozoic nodular cherts; evidence for opal-CT precursors and direct quartz replacement: American Journal of Science, v. 288, p. 798–809.
Maliva, R.G., and Siever, R., 1988b, Mechanism and controls of silicification of fossils in limestones: The Journal of Geology, v. 96, p. 387–398.
Mallard, E., 1890, Sur la lussatite, nouvelle variété minérale cristallisée de silice: Académie des Sciences (Paris), Comptes Rendus, v. 110, p. 245–247.
Marshall, W.L., and Warakomski, J.M., 1980, Amorphous silica solubilities. II Effect of aqueous salt solutions at 25°C: Geochimica et Cosmochimica Acta, v. 44, p. 915–924.
Michel-Levy, A., and Munier-Chalmas, E., 1892, Sur de nouvelles formes de silice cristallisée: Académie des Sciences (Paris), Comptes Rendus, v. 110, p. 649–652.
Milliken, K.L., 1979, The silicified evaporite syndrome: Two aspects of silification history of former evaporite nodules from southern Kentucky and northern Tennessee: Journal of Sedimentary Petrology, v. 49, p. 245–256.
Minguez, J.M., and Elorza, J., 1994, Diagenetic volume-for-volume replacement: force of crystallization and depression of dissolution: Mineralogical Magazine, v. 58, p. 135–142.
Nash, D.J., and Shaw, P.A., 1998, Silica and carbonate relationships in silcrete–calcrete intergrade duricrusts from the Kalahari of Botswana and Namibia: Journal of African Earth Sciences, v. 27, p. p. 11–25.
Owen, R.M., and Nasr, S.W., 1958, Stratigraphy of the Kuwait–Basrah area, *in* Weeks L.G., ed., Habitat of Oil: American Association of Petroleum Geologists, Bulletin, p. 1252–1278.
Pekar, S.F., and DeConto, R.M., 2006, High-resolution ice-volume estimates for the early Miocene: evidence for a dynamic ice sheet in Antarctica: Palaeogeography, Palaeoclimatology, Palaeoecology, v. 231, p. 101–109.
Powers, R.W., Ramibez, I.F., Redmond, C.D., and Elbebg, E.L., 1966, Sedimentary geology of Saudi Arabia, Geology of the Arabian Peninsula: U.S. Geological Survey, Professional Paper 560-D, 147 p.
Renaut, R.W., and Owen, R.B., 1992, Opaline cherts associated with sublacustrine hydrothermal springs at Lake Bogoria, Kenya Rift valley: Geology, v. 16, p. 699–702.
Rimstidt, J.D., 1997, Quartz solubility at low temperatures: Geochimica et Cosmochimica Acta, v. 61, p. 2553–2558.
Rodgers, K.A., Browne, P.R.L., Buddle, T.F., Cook, K.L., Greatrex, R.A., Hampton, W.A., Herdianita, N.R., Holland, G.R., Lynne, B.Y., Martin, R., Newton, Z., Pastars, D., Sannazarro, K.L., and Teece, C.I.A., 2004, Silica phases in sinters and residues from geothermal fields of New Zealand: Earth-Science Reviews, v. 66, p. 1–61.
Sander, N.J., 2012, Paleontologic and stratigraphic overview of the Paleogene in eastern Saudi Arabia: Notebooks on Geology, Brest, Article 2012/04 (CG2012_A04), p. 53–92.
Segnit, E.R., Anderson, C.A., and Jones, J.B., 1970, A scanning microscope study of the morphology of opal: Search, v. 1, p. 349–351.
Siffert, B., 1967, Some reactions of silica in solution: formation of clay. Translation of: Mémoires du Service de la Carte géologique d'Alsace et de Lorraine, no. 21: U.S. Department of Agriculture and the National Science Foundation, 100 p.
Singer, A., and Galan, E., 1984, Palygorskite–sepiolite occurrences, genesis and uses: Amsterdam, Elsevier, Developments in Sedimentolology 37, 352 p.
Storz, M., 1926, Zur petrogenesis des Sekundären Kieselgesteine in der Südlichen Namib, *in* Kaiser E., ed., Die Diamantenwüste Sudwest-Afrikas: Berlin, Dietrich Reimer, p. 254–282.
Tanoli, S., and Al-Bloushi, A., 2017, Depositional history of the Eocene Dammam Formation in Kuwait: Society of Petroleum Engineers, Kuwait Oil & Gas Show and Conference, 14 p., DOI: 10.2118/187628-MS.
Thiry, M., and Maréchal, B., 2001, Development of tightly cemented sandstone lenses within uncemented sand: example of the Fontainebleau Sand (Oligocene) in the Paris Basin: Journal of Sedimentary Research, v. 71, p. 473–483.
Thiry, M., and Millot, G., 1987, Mineralogical forms of silica and their sequence of formation in silcretes: Journal of Sedimentary Petrology, v. 57, p. 343–352.
Thiry, M., and Milnes, A.R., 1991, Pedogenic and groundwater silcretes at Stuart Creek Opal Fields, South Australia: Journal of Sedimentary Petrology, v. 61, p. 111–127.
Thiry, M., and Milnes, A., 2017, Silcretes: insights into the occurrences and formation of materials sourced for stone tool making: Journal of Archaeological Sciences: Reports, v. 15, p. 500–513.

Thiry, M., and Ribet, I., 1999, Groundwater silicifications in Paris Basin limestones: fabrics, mechanisms, and modeling: Journal of Sedimentary Research, v. 69, p. 171–183.

Thiry, M., Bertrand-Ayrault, M., and Grisoni, J.-C., 1988, Ground-water silicification and leaching in sands: example of Fontainebleau Sand (Oligocene) in the Paris Basin: Geological Society of America, Bulletin, v. 100, p. 1283–1290.

Thiry, M., Milnes, A.R., Rayot, V., and Simon-Coinçon, R., 2006, Interpretation of palaeoweathering features and successive silicifications in the Tertiary regolith of Inland Australia: Geological Society of London, Journal, v. 163, p. 723–736.

Thiry, M., Millot, R., Innocent, C., and Franke, C., 2015a, The Fontainebleau Sandstone: bleaching, silicification and calcite precipitation under periglacial conditions: Orléans, France, Applied Isotope Geochemistry Conference, Field Trip Guide, Scientific Report, no. RS150901MTHI, 26 p.

Thiry, M., Milnes, A., and Ben Brahim, M., 2015b, Pleistocene cold climate groundwater silicification, Jbel Ghassoul region, Missour Basin, Morocco: Geological Society of London, Journal, v. 172, p. 125–137.

Van Tuyl, F.M., 1918, The origin of chert: American Journal of Science, v. 270, p. 449–456.

White, D.E., Hem, J.D., and Waring, G.A., 1963, Chemical composition of subsurface waters, *in* Fleischer, M., ed., Data of Geochemistry, 6th Edition: U.S. Geological Survey, Professional Paper 440-F, 66 p.

Willey, J.D., 1980, Effects of ageing on silica solubility: a laboratory study: Geochimica et Cosmochimica Acta, v. 44, p. 573–578.

Williams, L.A., and Crerar, D.A., 1985, Silica diagenesis, II General mechanisms: Journal of Sedimentary Petrology, v. 55, p. 312–321.

Williams, L.A., Parks, G.A., and Crerar, D.A., 1985, Silica diagenesis, I. Solubility controls: Journal of Sedimentary Petrology, v. 55, p. 301–311.

Zachos, J.C., Pagani, M., Sloan, L., Thomas, E., and Billups, K., 2001a, Trends, rhythms, and aberrations in global Climate 65 Ma to Present: Science, v. 292, p. 686–693.

Zachos, J.C., Shackleton, N.J., Revenaugh, J.S., Pälike, H., and Flower, B.P., 2001b, Climate response to orbital forcing across the Oligocene–Miocene boundary: Science, v. 292, p. 274–278.

Received 1 March 2019; accepted 11 December 2019.